Proton Transfer Assisted Charge Transfer Phenomena in Photochromic Schiff Bases and Effect of −NEt2 Groups to the Anil Schiff Bases

ARTICLE *in* THE JOURNAL OF PHYSICAL CHEMISTRY A · OCTOBER 2012

Impact Factor: 2.69 · DOI: 10.1021/jp3079698 · Source: PubMed

3 AUTHORS, INCLUDING:

Sankar Jana
Tohoku University

33 PUBLICATIONS **352** CITATIONS

SEE PROFILE

THE JOURNAL OF PHYSICAL CHEMISTRY A

Article

pubs.acs.org/JPCA

Proton Transfer Assisted Charge Transfer Phenomena in Photochromic Schiff Bases and Effect of $-NEt_2$ Groups to the Anil Schiff Bases

Sankar Jana, Sasanka Dalapati, and Nikhil Guchhait*

Department of Chemistry, University of Calcutta, 92 A.P.C. Road, Kolkata-700009, India

Supporting Information

ABSTRACT: Photochromic Schiff bases 5-diethylamino-2-[(4-diethylamino-benzylidene)-hydrazonomethyl]-phenol (DDBHP) and *N*,*N*′-bis(4-*N*,*N*-diethylaminosalisalidene) hydrazine (DEASH) with both the proton and charge transfer moieties have been synthesized, and their photophysical properties such as excited state intramolecular charge transfer (ICT) and proton transfer (ESIPT) processes have been reported on the basis of steady-state and time-resolved spectral measurement in various solvents. The ground-state six-membered intramolecular hydrogen bonding network at the proton transfer site accelerates the ESIPT process for these compounds. Both the compounds show large Stokes-shifted emission bands for proton transfer and charge transfer processes. The hydrogen bonding solvents play a crucial role in these photophysical processes. Excited-state dipole moment of DDBHP and DEASH calculated by the solvatochromic method supports the polar character of the charge transfer excited state. Introduction of $-NEt_2$ groups to the reported salicylaldehyde azine (SAA) Schiff base results an increase in fluorescence lifetime from femtosecond to picosecond time scale for the proton transfer process.

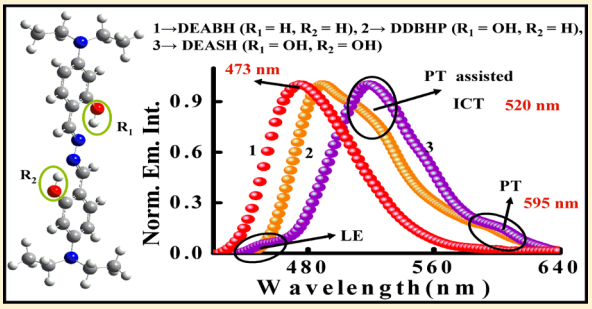

1. INTRODUCTION

For years, Schiff bases have been widely used for toxic and essential ion sensors,[1−3] molecular memories and switches,[4] nonlinear devices,[5] catalysis,[6] electrochemistry,[7] magneto-chemistry,[8] asymmetric synthesis, epoxidation,[9] molecular separation, biomedical applications,[10] and so on. There are two main reasons for extensive studies on Schiff bases. First, Schiff bases can easily be prepared through a one-step synthetic procedure via condensation of aldehydes with amines. Second, Schiff bases derived from salicylaldehyde derivatives having 2-hydroxy group are of interest mainly due to the existence of O−H···N and O···H−N type hydrogen bonds, which undergo excited state tautomerization between enol-imine and keto-enamine forms.[11−14]

On the other hand, photoinduced intramolecular charge transfer (ICT) process and the subsequent dual fluorescence in molecules with donor-chromophore-acceptor groups[15−17] find importance in various applications such as pH and ion detectors, thin film transistors, electro-optical switches, solar cells, and the creation of new optoelectronic devices such as electroluminescence devices and[15,18,19] chemical sensors for free volume measurement in polymers, probes for the study of microheterogeneous environments,[20,21] degree of water penetration into the surfactant aggregates, and sensing the local polarity of the microenvironment at binding sites on proteins.[21−23] These charge transfer molecules also have a crucial role in biological light harvesting processes such as photosynthesis.[24] At the same time, the phenomenon of excited state intramolecular proton transfer (ESIPT)[25] has been extensively investigated over the past few decades due to their interesting photophysical and photochemical properties and their vast applications in the field of biochemistry, analytical chemistry, electrochromic modulation, perturbation of electronic state by variation of solvent polarity, laser dyes, molecular memory storage devices, fluorescence probes, polymer protectors, metabolic process of living systems, and so on.[26−32]

It is found in the literature that Schiff bases, ICT, and PT molecules have wide range of applications. But when both the ICT and PT properties are combined in a single Schiff base molecule, it is expected that their utility and applications will be magnified manifold. For this purpose, we have changed the so-called reported anils Schiff bases (salicylaldehyde with amines) by introducing two additional $-NEt_2$ groups and have considered 5-diethylamino-2-[(4-diethylamino-benzylidene)-hydrazonomethyl]-phenol (DDBHP) and *N*,*N*′-bis(4-*N*,*N*-diethylaminosalisalidene)hydrazine (DEASH) Schiff base molecules, which can show additional ICT reaction with the so-called reported PT reaction. Recently, the ESIPT reaction has been studied in a number of interesting photochromic Schiff bases by various research groups[33−41] but until now, there have been no such reports of anil Schiff base where both the ICT

Received: August 10, 2012
Revised: October 16, 2012
Published: October 25, 2012

   dx.doi.org/10.1021/jp3079698 | *J. Phys. Chem. A* 2012, 116, 10948−10958

and PT processes occur simultaneously in a single Schiff base molecule.

Here, we report the photophysical properties of DDBHP and DEASH (Scheme 1) molecules. We have chosen DDBHP and DEASH molecules for studying the photophysical properties because these molecules have widely been used as effective sensors for heavy, essential, and toxic metal ions.[1,42,43] Here, the photophysical properties (coupled ESIPT and ICT) of DDBHP and DEASH molecules have been reported on the basis of steady-state spectroscopy, quantum yield calculation, time-resolved measurement with variation of polarity and hydrogen bonding ability of solvents. Calculation of ground- and excited-state dipole moments and polarity-dependent Stokes shift helps us to establish the occurrence of ICT and PT processes and the effect of hydrogen bonding solvents on these processes. At the same time, we have compared the effect of $-NEt_2$ group on the photophysical properties of anil Schiff bases on the basis of absorption and emission band position, Stokes shift, quantum yields, fluorescence lifetime, and emission intensity.

Scheme 1. Energy Optimized Structure of (a) DDBHP and (b) DEASH Using the DFT Method and 6-311+G(*d,p*) Basis Set with the Help of Gaussion 03 Software[a]

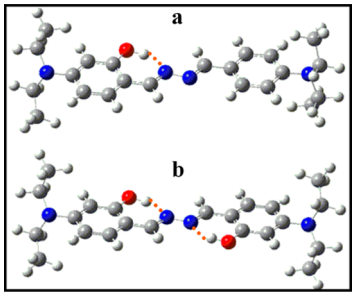

[a]The dotted lines are hydrogen bonding interactions.

2. EXPERIMENTAL DETAILS

2.1. Chemicals. The synthetic procedure and purification of DDBHP and DEASH (Scheme 1) were mentioned in our earlier publications.[42,43] Spectroscopic grade solvents and trifluoroacetic acid (TFA) were purchased from Spectrochem India Pvt. Ltd. and were used after proper distillation as needed. Ethanol, sulfuric acid, and triethylamine (Et_3N) from E. Merck were used as received. Sodium hydroxide was purchased from SRL India Pvt., Ltd. Triple-distilled water was used for the preparation of all aqueous solutions. Abbreviations of all the solvents used are given in the Supporting Information.

2.2. Steady State Spectral Measurements. All the spectral measurements were done within an $\sim 10^{-6}$ to 10^{-7} M concentration range of solute in order to avoid aggregation and self-quenching. The steady-state absorption spectra of DDBHP and DEASH were recorded by a Hitachi UV−vis U-3501 spectrophotometer. Emission spectra were recorded by a Perkin-Elmer LS55 fluorescence spectrophotometer equipped with a 10 mm quartz cell and a thermostat bath at 298 K temperature.

The fluorescence quantum yield of DDBHP and DEASH in solvents having different polarity were measured relative to anthracene in EtOH (Φ_f = 0.27) as a secondary standard and calculated on the basis of the following equation:[16,44,45]

$$\Phi_f = \Phi_f^0 \frac{n^2 A^0 \int I_f(\lambda_f)\, d\lambda_f}{n_0^2 A \int I_f^0(\lambda_f)\, d\lambda_f} \quad (1)$$

Where n_0 and n are the refractive index of the solvents, A^0 and A are the absorbances, Φ_f^0 and Φ_f are the fluorescence quantum yields, and the integrals denote the area of the fluorescence band for the standard and the sample, respectively.

2.3. Measurement of Time-Resolved Emission Spectra. Fluorescence lifetimes were measured from time-resolved intensity decay by the method of time correlated single-photon counting (TCSPC) on a FluoroCube-01-NL spectrometer (Horiba Jobin Yovon IBH Ltd.) using a laser source at 375 nm, and the signals were collected at the magic angle (54.7^o) polarization. The IRF of the detector is (fwhm) = 130 ps. The DAS6 software was used to deconvolute the fluorescence decays. The relative contribution of each component was obtained from the biexponential fitting finally and expressed by the following equation:[2,22]

$$a_n = \frac{B_n}{\sum_{i=1}^{N} B_i} \quad (2)$$

B_i is the pre-exponential factor. The mean fluorescence lifetimes for the decay curves were calculated from the decay times and the relative contribution of the components using the following equation:

$$\langle \tau \rangle = \frac{\sum a_i \tau_i^2}{\sum a_i \tau_i} \quad (3)$$

τ_i and a_i are the fluorescence lifetime and its coefficient of the ith component, respectively.

3. RESULTS AND DISCUSSION

3.1. Absorption Spectra. The absorption profile of DDBHP ($\sim 10^{-6}$ M) with varying solvent polarity and hydrogen bonding ability is shown in Figure 1a, and all the spectral band maxima are listed in Table 1. DDBHP shows a broad absorption band at ~395 nm in nonpolar solvents with a shoulder at ~415 nm. In the case of polar protic and aprotic solvents, the same absorption band appears at ~410 nm. The molecule DEASH shows a similar but slightly red-shifted absorption band at ~407 nm in nonpolar solvents such as *n*-hept, CY, CCl_4, and so on (Figure 1b). However, in the case of polar protic and polar aprotic solvents, DEASH shows the same absorption band position at and around ~415 nm. Compared to the earlier reported similar types of systems, the absorption band within ~400−420 nm can be assigned to the $S_0(n) \rightarrow S_1(\pi^*)$ type of electronic transition.[12]

3.2. Steady-State Emission and Excitation Spectra. The steady state emission spectra of DDBHP were recorded in different solvents by exciting at the respective absorption maxima and are shown in Figure 2a. The emission spectral data are also provided in Table 1. Since DDBHP contains both the charge and proton transfer moieties, there are the possibilities of observing charge transfer (CT), proton transfer (PT) and local emission (LE) bands. As seen in Figure 2a, DDBHP shows peaks at ~458 and ~500 nm in nonpolar solvent. At this stage, it is really hard to precisely assign this broad double-hump band, as the reported literature on similar systems is really confusing. Das et al.[46] reported a similar type of structured band in quinoline-based azine Schiff base, and they claimed that the origin of the structure band is due to syn−anti

dx.doi.org/10.1021/jp3079698 | J. Phys. Chem. A 2012, 116, 10948−10958

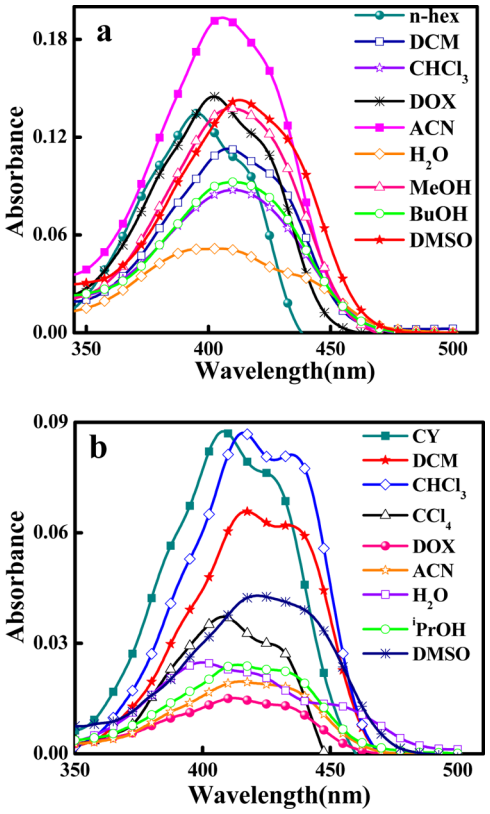

Figure 1. Absorption spectra of (a) DDBHP and (b) DEASH in different solvents with varying polarities and hydrogen bonding abilities at 298 K temperature.

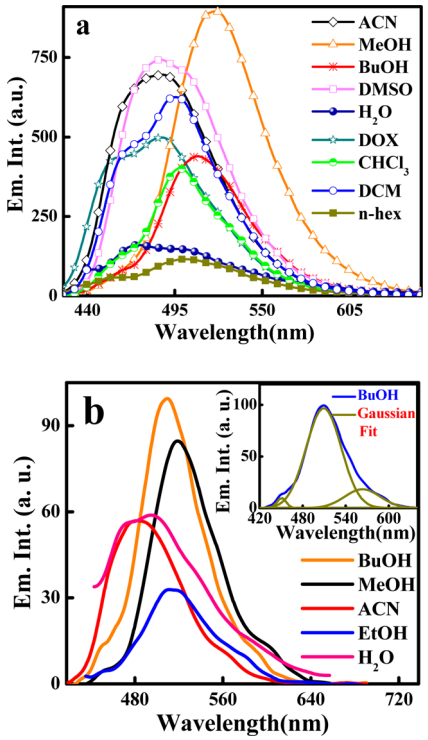

Figure 2. (a) Emission spectra of DDBHP in different solvents with variation of polarity and hydrogen bonding ability at room temperature. (b) PT and CT emission bands of DDBHP; inset: Gaussian fit of the emission spectra of DDBHP in BuOH solvent.

isomerization around the C═N bond. A similar conclusion was suggested by Mukherjee et al.[47] and Zein et al.[48] in the case of 7-ethylsalicylidenebenzylamine (ESBA) and salicylideneaniline (SA) Schiff bases, respectively. On the other hand, Rentzepis et al.[41] explained this as vibrational relaxation of the cis keto form via C_1-C_7 single bond rotation of SA (C_1 is the carbon atom of the benzene ring, and C_7 is the carbon atom of the C═N bond). Maciejewski et al.[49] reported the same phenomenon by the open trans enol structure (with respect to the C−C (phenol) bond) and closed (with an intramolecular hydrogen bond) enol tautomers of SAA. Here we have assigned the high energy band at ∼458 nm to the open form of the enol tautomer and ∼500 nm to the closed form of the enol tauomer, which is more stable due to intramolecular hydrogen bonding.[36,50] With increasing slight polarity of solvents such as dichloromethane

Table 1. Steady-State Spectroscopic Parameters Obtained from Absorption and Emission Spectra of DDBHP and DEASH in Different Solvents at Room Temperature[a]

	λ_{abs}(nm)		λ_{flu}(nm)		$\Delta\nu$(cm^{-1})		Φ	
solvent	DDBHP	DEASH	DDBHP	DEASH	DDBHP	DEASH	DDBHP	DEASH
n-hept	393, 415	406, 427	499, 458	450, 474	3611	2408	0.374	0.096
n-hex	395, 413	425	505, 458	450, 475	3482	2469	0.372	0.112
MCH	396, 416	429	491, 457	453, 474	3370	2494	0.358	0.188
CY	396, 415	408, 426	498, 462	450, 475	3607	2287	0.421	0.100
CCl_4	401, 422	409, 428	498, 456	583, 460, 487	3007	7297, 2710	0.423	0.287
DCM	408, 428	417, 435	495, 467	473, 504	4307	2839	0.245	0.361
$CHCl_3$	411	416, 435	498, 469	499, 471	4250	3998	0.243	0.295
DOX	420	412, 434	486, 458	542, 465, 487	4299	5821, 2766	0.034	0.227
DMF	409	423	482	553, 481	3702	5557, 2850	0.026	0.076
DMSO	413	420, 440	482, 506	485	4450	3190	0.049	0.115
ACN	406	413, 436	565, 489	477	6931, 4180	3248	0.016	0.232
^{i}PrOH	410	411, 435	506, 458	507, 465	4627	4607	0.331	0.283
BuOH	410	413, 435	579, 510, 466	512, 467	7119, 4782	4681	0.354	0.385
EtOH	411	414, 432	582, 515	514, 465	7148, 4913	4699	0.490	0.424
MeOH	410	412, 434	595, 520, 466	518, 470	7583, 5159	4966	0.504	0.454
H_2O	436	401, 425, 458	600, 470, 508	592, 486, 517	8208, 3599	8045, 5595	0.070	0.019

[a] λ_{abs}, λ_{flu}, $\Delta\nu$, and Φ are absorption, emission band position, Stokes shift, and fluorescence quantum yield, respectively.

dx.doi.org/10.1021/jp3079698 | J. Phys. Chem. A 2012, 116, 10948−10958

(DCM), $CHCl_3$ and 1,4-dioxane (DOX), the nature of the emission band is found to be similar to that in the case of nonpolar solvent, but here the low energy band appears within the 486−495 nm wavelength range depending upon the polarity of solvents (Figure 2a). Therefore, the polarity-dependent emission band (486−495 nm) is assigned to the CT band,[16,17,36] and the higher energy band at ∼465 nm is the LE band. The DDBHP molecule contains both PT and CT possibilities, where CT may occur from the $-NEt_2$ group to the −CH═N− moiety, which acts as an acceptor. For polar protic solvent, the shoulder nature of the band vanishes, and a sharp emission band appears within the 505−520 nm range with two additional peaks: one at ∼462 nm and another red-shifted low energy band at ∼595 nm (Figure 2b). Compared to similar reported systems, here we have assigned the ∼595 nm band as the PT band ($\pi \rightarrow \pi^*$).[34,36,39] The polarity-sensitive band up to 520 nm has been assigned to the CT band,[36] which is observed due to the excited state ICT from the donor $-NEt_2$ group to the acceptor part of the CT moiety (−CH═N−), which acts as a better acceptor in the PT case and facilitates the PT process as the electron density on the N atom of the acceptor part becomes higher after CT or vice versa, i.e., after PT, the slight increase in positive charge density will increase the acceptor strength, and, as a result, CT is facilitated. For easy and safe assignment of the CT emission band, we have also recorded the emission spectra of *N*,*N*′-bis-[4-*N*,*N*-diethylaminobenzylidene]-hydrazine (DEABH) (Scheme S1, Supporting Information) in polar solvent where the possibility of proton transfer is absent, but there is a possibility of CT. Here the CT band was not observed [no such polarity-dependent and large Stokes-shifted emission band, λ_{em} = 473 (MeOH), 468 (EtOH), 467 nm (BuOH)], which indicates that, in the absence of PT moiety, the CT process is not possible. Therefore, it is clear that PT process facilitates the CT phenomenon. As seen in Figure 2b, for the DDBHP molecule, the maxima of the PT band varies with polarity and hydrogen bonding ability of the solvent (PT emission in acetonitrile (ACN) solvent is at 565 nm, and it is within the range of 579−600 nm in ^{i}PrOH to H_2O). The variation of the position of the PT emission band in protic solvents indicates the influence of intermolecular hydrogen bonding on the PT reaction.[12,37,51] For clear observation of the LE, CT, and PT emission bands, we have shown the emission spectra of DDBHP in BuOH solvent and its Gaussian fitted spectra in Figure 2b (inset).

On the other hand, for DEASH, there is a possibility of double proton transfer due to the presence of two −OH functional groups. Here the emission spectral pattern (Figure 3a) is also similar to that of DDBHP, where the LE arises within 450−465 nm, and CT emission was observed within 485−518 nm with variation of the solvent polarity and hydrogen bonding ability of the solvent. The proton transfer band appears at ∼550−595 nm (Figure 3b). Compared to the earlier reported similar types of systems and also with DDBHP, it is clear that double PT is not observed in the case of DEASH.[49,52,53]

The excitation spectra of DDBHP by monitoring both the low- and high-energy emission bands (LE and CT) are the same (Figure S1a) except for the difference in intensity. It is seen that the excitation spectra of DDBHP in different solvents resemble the absorption spectra (Figure 1a). The similarity between excitation and absorption spectra indicates the origin of LE (enol), PT (keto), and CT emission through the excitation of the same ground-state species.[54,55] The excitation

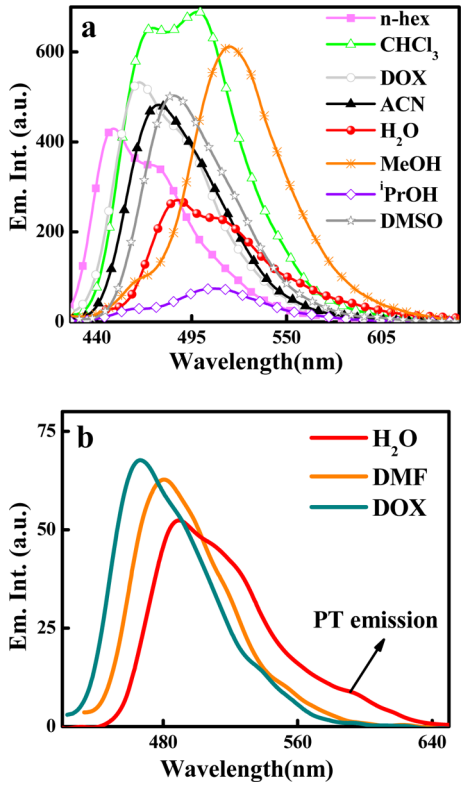

Figure 3. (a) Emission spectra of DEASH in different solvents with variation of polarity and hydrogen bonding ability at 298 K temperature. (b) PT and CT emission bands of DEASH.

spectra of DEASH is also similar in nature to that of the DDBHP when monitoring both the low and high energy emission bands (Figure S1b). Here also the similar nature of excitation spectra with that of the absorption spectra of DEASH supports that the LE, CT, and PT emissions originate from the same species in the ground state.[54,56]

3.3. Effect of Acid on Combined ICT and PT Processes.

To know more details about the absorption and emission bands, we have recorded the absorption and emission spectra for both the molecules with variation of pH in MeOH and ACN solvent. Figure 4 represents the absorption spectra of DDBHP with increasing H_2SO_4 acid concentration in MeOH solvent. DDBHP shows absorption maxima at ∼410 nm in MeOH solvent. During titration when acid concentration is very low, the absorption band at ∼410 nm decreases with the generation of a new band at ∼480 nm through an isosbestic point at 437 nm (Figure 4a). With further increase of acid concentration, the absorption band at ∼480 nm is found to be shifted to ∼445 nm with decrease in absorbance values (Figure 4b). Initially, at very low concentration of acid, protonation takes place at the N atom of $-NEt_2$ group, which forms monocationic species of DDBHP (Scheme 2a) and shows absorbance at ∼480 nm.[42,43] The red shift of the absorption maxima is due the delocalization of the lone pair electron on the N atom of the neutral part of $-NEt_2$ to the protonated positively charged $-NEt_2$ part of DDBHP and also by the stabilization of the dipolar molecule in polar MeOH solvent.[43] Further increase of acid concentration generates dicationic species from the monocation (Scheme 2b), which shows an absorption band at ∼445 nm. Since the dicationic species is less stable compared to that of the monocationic species due to the absence of resonance delocalization, blue shifting of the

dx.doi.org/10.1021/jp3079698 | J. Phys. Chem. A 2012, 116, 10948−10958

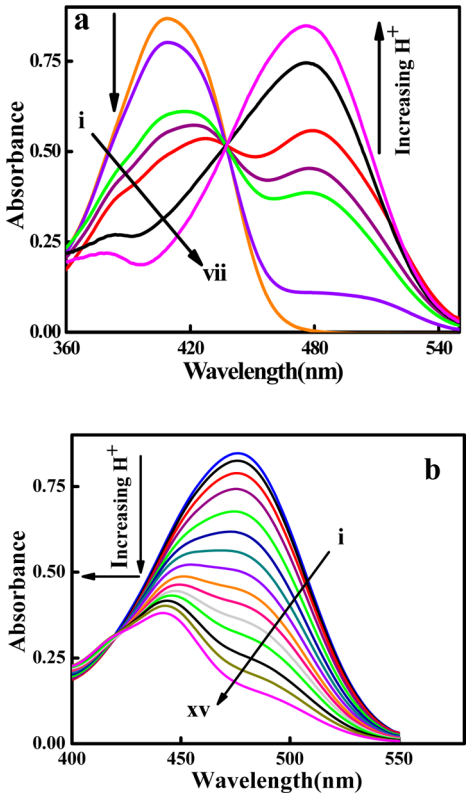

Figure 4. Effect of acid on steady-state absorption spectra of DDBHP in (a) low (i→vii; 0, 36, 90, 130, 200, 250, 300 μM H_2SO_4) and (b) high (i→xv; 0.3, 0.6, 0.9, 1.2, 1.5, 1.8, 2.2, 2.5, 2.8, 3.1, 3.4, 3.7, 3.8, 4.1, 4.4 mM) concentration of H_2SO_4 in MeOH solvent.

Scheme 2. (a) Monocationic and (b) Dicationic Form of DDBHP in the Presence of H_2SO_4 in MeOH Solvent

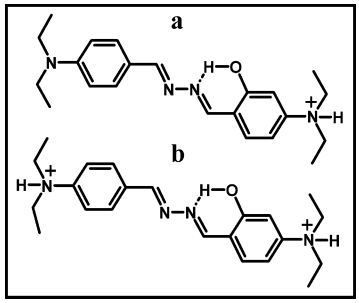

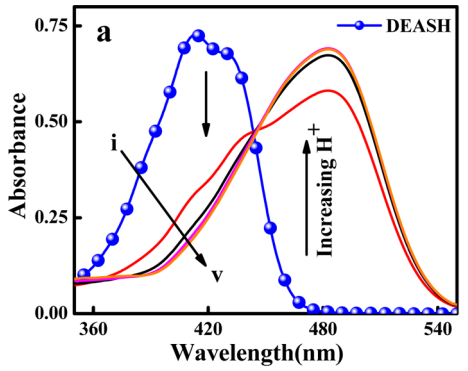

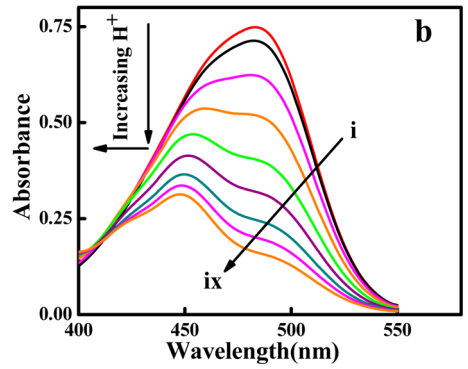

Figure 5. Effect of acid on steady-state absorption spectra of DEASH in (a) low (i→v; 0, 27, 50, 80, 130 μM H_2SO_4) and (b) high (i→ix; 13, 16, 19, 22, 25, 28, 31, 34, 41 × 10^{-4} M) concentration of H_2SO_4 in MeOH solvent.

Scheme 3. (a) Monocationic and (b) Dicationic Form of DEASH in the Presence of H_2SO_4 in MeOH Solvent

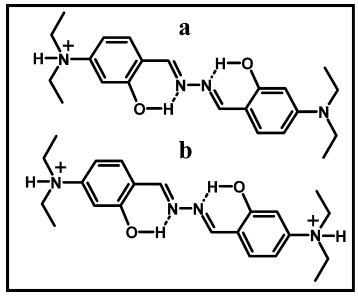

absorption maxima of the dicationic species with respect to the monocationic species is observed. Since the absorption band of DDBHP at ~410 nm vanishes, it is clear that the absorption band is originated due to the n → π^* type of electronic transition.[16,17] The protonation at the N atom of $-NEt_2$ groups is confirmed from the acid effect of the SAA molecule in MeOH solvent where no $-NEt_2$ group is present. It is found that SAA did not show such types of absorption bands in the presence of acid. Under similar experimental conditions, DEASH also shows similar absorption spectral changes in the presence of H_2SO_4 in MeOH solvent. It also shows an absorption band for monocationic (Figure 5a, Scheme 3a) and dicationic (Figure 5b, Scheme 3b) species at ~484 and ~448 nm, respectively, whereas the bare molecule itself shows absorption band maxima at ~412 nm.

The emission spectra of DDBHP have been recorded with increasing acid concentration in MeOH solvent. The DDBHP molecule shows emission band maxima at ~520 nm in MeOH (Figure 6a). With increase of H_2SO_4 acid concentration, the emission band suddenly decreases its intensity and is red-shifted to ~533 nm while emission intensity tends to zero. Here the disappearance of the emission band with increasing acid concentration indicates that the CT emission band originates from the n → π^* type of electronic transition, and this CT band disappears due to protonation of $-NEt_2$ group in the presence of acid.[16,17] The final protonated species is stabilized in polar MeOH solvent, which causes the red shift of the resultant emission spectra. As shown in Figure 6b, DEASH also shows similar emission spectral changes with that of the emission spectra of DDBHP in the presence of H_2SO_4 in MeOH solvent. Here also the emission band at ~518 nm of the bare DEASH molecule was shifted to ~532 nm with a decrease in emission intensity in the presence of acid. Formation of monocationic and dicationic species in the presence of acid was confirmed by excitation at the mono (λ_{ex} = 480 nm) and

dx.doi.org/10.1021/jp3079698 | J. Phys. Chem. A 2012, 116, 10948−10958

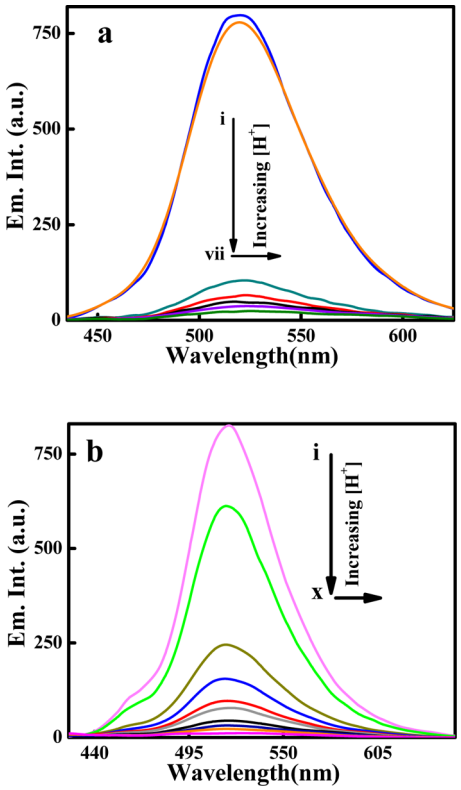

Figure 6. Effect of acid on steady state emission spectra of (a) DDBHP (i→vii; 0, 0.18, 0.5, 0.9, 1.2, 1.4, 1.6, 1.8 mM H_2SO_4) and (b) DEASH (i→x; 0, 0.06, 0.21, 0.36, 0.51, 0.66, 0.81, 0.91, 0.98, 1.05 mM) concentration of H_2SO_4 in MeOH solvent.

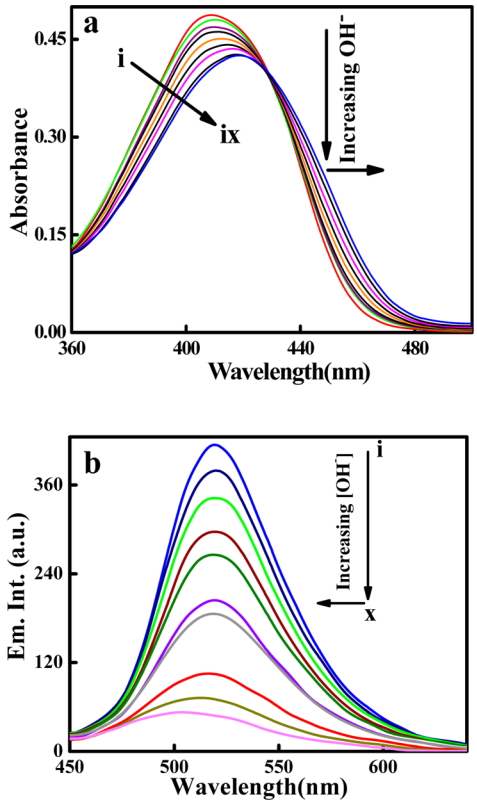

Figure 7. Effect of base on steady state (a) absorption (i→ix; 0, 2.1, 5.3, 8.6, 11.7, 15.4, 20.8, 31.2, 40 mM NaOH) and (b) emission (i→x; 0, 2.3, 4.1, 6.7, 9.3, 12.5, 16.4, 19.7, 22, 25.3 mM NaOH) spectra of DDBHP with increasing NaOH concentration in MeOH solvent.

dicationic (λ_{ex} = 445 nm) absorption maxima, and the emission bands were observed at ∼552 and ∼533 nm for monocationic and dicationic species, respectively.

To avoid any hydrogen bonding solvent effect on the protonation process, we also recorded the absorption and emission spectra in ACN solvent in the presence of TFA. Here similar types of absorption spectra have also been observed (Figure S2). DDBHP molecule shows an absorption band at ∼406 nm in ACN solvent, and in the presence of TFA it shows absorption bands of monocationic (Figure S2a) and dicationic (Figure S2b) species at ∼483 and ∼443 nm, respectively. When emission spectra were recorded in ACN solvent as a function of TFA concentration, it also shows a nature (Figure S3) similar to that of the emission spectra of DDBHP in the presence of H_2SO_4 in MeOH solvent (Figure 6a). DEASH shows similar types of monocationic (Figure S4a) and dicationic (Figure S4b) absorption and emission band maxima (Figure S5) at ∼483, ∼448 and ∼527 nm, respectively.

3.4. Effect of Base on Steady-State Absorption and Emission Spectra. To support the phenomenon of PT and ICT processes in DDBHP and DEASH, the steady-state absorption and emission spectra have also been recorded in the presence of base in MeOH and ACN solvents.[17,50] Upon addition of methanolic solution of NaOH to the methanolic solution of DDBHP, the original absorption band at ∼410 nm shifts to the red side (∼420 nm) with decreasing absorbance (Figure 7a). The final absorption band at ∼420 nm is the absorbance of the anion which is formed by the deportation of the −OH proton in the presence of strong base NaOH. The red shifting is due to the delocalization of the negative charge after formation of the anion.[50,57] Similarly, when emission spectra were recorded with increasing NaOH concentration, the emission band of the bare DDBHP molecule at ∼520 nm gradually blue-shifted to ∼506 nm with concomitant decrease in emission intensity (Figure 7b). Here the band at ∼506 nm is generated from the emission of anion of the bare molecule. The blue shifting of the emission band in the presence of base is due to the breaking of six-member intramolecular hydrogen bonds, which result in an increase in energy of the anion of DDBHP or may be due to destabilization of the excited state anion through CT where there is repulsion between the negative charge of the anion and the transferred charge on the acceptor group after the ICT process.[50] To avoid any hydrogen bonding effect on the deprotonation process, we also recorded the absorption and emission spectra in ACN solvent in the presence of Et_3N. Since Et_3N is a weak and bulky base, it is unable to abstract the −HO proton by breaking of the cyclic six-membered intramolecular hydrogen bond.[50] Therefore, we have not observed any characteristic absorption and emission spectral change on addition of base Et_3N. In the case of DEASH with increasing NaOH concentration in MeOH solvent, the original absorption band at ∼412 nm is red-shifted to ∼430 nm with slight decrease in absorbance (Figure 8a). The absorption band at ∼430 nm has been assigned as the anion of DEASH. The emission spectral profile (λ_{ex} = 412 nm) (Figure 8b) with increasing NaOH concentration shows a progressive decrease in intensity of the original emission band (∼518 nm) of DEASH in MeOH solvent. The final emission band at ∼518 nm is nothing but the emission from the anion of DEASH.

3.5. Excited State Polarity and Effect of Solvent. The high dipolar character of the emissive species can be

dx.doi.org/10.1021/jp3079698 | J. Phys. Chem. A 2012, 116, 10948−10958

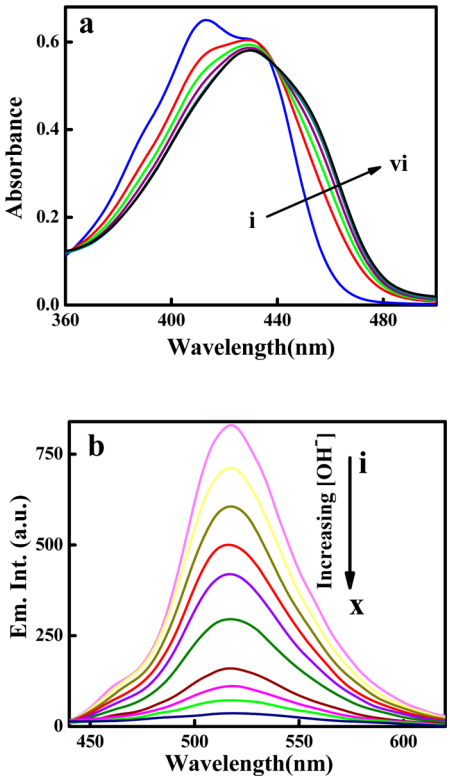

Figure 8. Effect of base on steady state (a) absorption (i→vi; 0, 3.5, 7.4, 15.8, 31.2, 53.5 mM) and (b) emission (i→x; 0, 3.5, 6.8, 9.5, 12.7, 16.4, 20.6, 26.8, 30.4 36.2 mM) spectra of DEASH with increasing NaOH concentration in MeOH solvent.

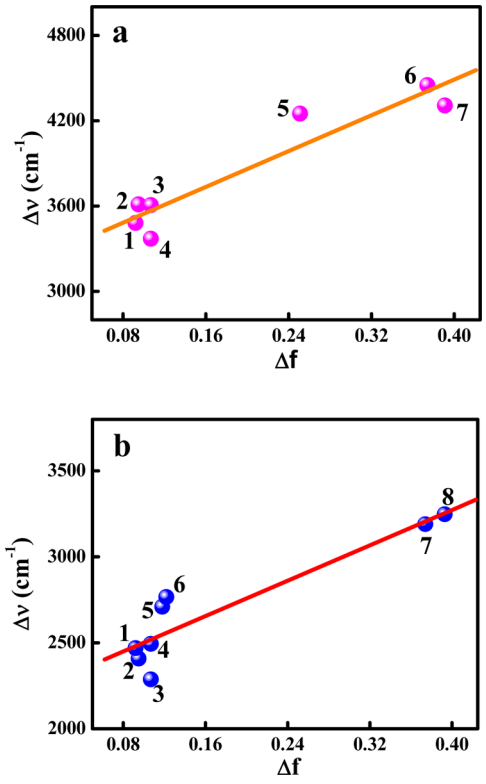

Figure 9. Plot of Stokes shift ($\Delta\nu$) against solvent parameter (Δf) for (a) DDBHP (1→7; *n*-hex, *n*-hept, CY, MCH, $CHCl_3$, DMSO, and DCM solvents, respectively) and (b) DEASH (1→8; *n*-hex, *n*-hept, CY, MCH, CCl_4, DOX, DMSO, and ACN solvents, respectively) molecule.

rationalized by solvatochromic shift of the CT emission band maxima and by the change in excited state dipole moment from that of the ground state. With increasing polarity of solvent, the CT band of DDBHP is shifted more to the red because the solvent dipoles orient themselves around the fluorophore to attain an energetically favorable arrangement, thereby stabilizing the polar CT state.[17,58] The excited state dipole moment has been calculated from the the slope of the Lippert−Mataga plot (Stokes shift ($\Delta\nu$) vs solvent parameter $\Delta f(\varepsilon_r,n)$) as shown in Figure 9a. The following Lippert−Mataga relation is used for calculating excited state dipole moment of the molecules:[59]

$$\nu_a - \nu_f = \frac{(\mu^* - \mu)^2}{2\pi\varepsilon_0 hc\rho^3} \times f(\varepsilon_r, n)$$

where

$$f(\varepsilon_r, n) = \left[\frac{\varepsilon_r - 1}{2\varepsilon_r + 1}\right] - \left[\frac{n^2 - 1}{2n^2 + 1}\right]$$

ν_a, ν_f, ε_r, and n are the absorption and emission band positions in cm^{-1}, the dielectric constant, and the refractive index of the medium, respectively. The terms h, ε_0, c, ρ, μ^*, and μ in the given equation are the Planck constant (6.626×10^{-34} J s), the permittivity of vacuum (8.85×10^{-34} V C^{-1} m^{-1}), the velocity of light ($3 \times 10^8 ms^{-1}$), the Onsagar cavity radius, and the ground- and excited-state dipole moments, respectively. It is found that the Lippert−Mataga plot shows linearity for nonpolar and polar aprotic solvents. The value of the Onsagar cavity radius (ρ) was calculated to be 5.97 Å by a volume test of the optimized structure of DDBHP at the density functional theory (DFT) level using the B3LYP functional and 6-311+G(d,p) basis set with the help of Gaussian 03 software.[60] From the ratio of the slope obtained from the Lippert plot and calculated values of ρ and μ, the excited state dipole moment has been calculated to be 9.40 D. The difference in the dipole moment ($\Delta\mu$ = 8.15 D) from the ground state (μ = 1.25 D) to the excited state (μ^* = 9.40 D) could only be possible by redistribution of charge in the excited-state surface by the intramolecular CT process from the $-NEt_2$ group to the −CH═N− acceptor group upon photo excitation. Also, by using a similar method (Figure 9b), the excited state dipole moment of DEASH has been calculated to be 7.08 D (μ^*). Here we have used the ground-state dipole moment =0.03 D and Onsagar cavity radius (ρ) = 5.80 Å , which were obtained from theoretical calculations using the same method and the same basis set we applied in the DDBHP molecule. Therefore, the large difference in dipole moment ($\Delta\mu$ = 7.05 D) between the ground and excited state of DEASH also suggests the same CT phenomenon as that of the DDBHP. However, in the case of the protic solvents, a deviation from linearity was observed in Lippert−Mataga plot, which indicates that the hydrogen bonding solvents have different types of influence on the nature of the CT state[16,17,61] of both the DDBHP and DEASH molecules.

To investigate the hydrogen bonding effect on the excited state ICT process, we have recorded the emission spectra of DDBHP with increasing hydrogen bonding ability of solvent, and the normalized emission spectra are presented in Figure 10a. For further information about the effect of hydrogen bonding, we have plotted the position of the emission band maxima (ν_f cm^{-1}) of DDBHP versus hydrogen bonding

dx.doi.org/10.1021/jp3079698 | J. Phys. Chem. A 2012, 116, 10948−10958

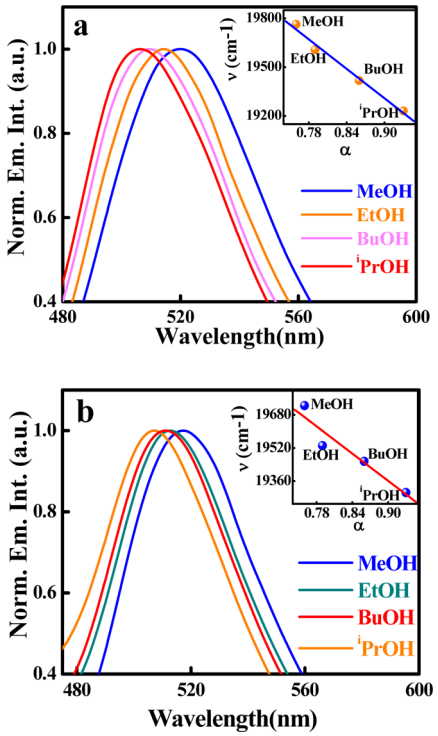

Figure 10. Normalize emission spectra of (a) DDBHP and (b) DEASH in different hydrogen bonding solvents. Inset shows the corresponding emission band maxima against the hydrogen bonding parameter (α) for hydrogen bonding solvents.

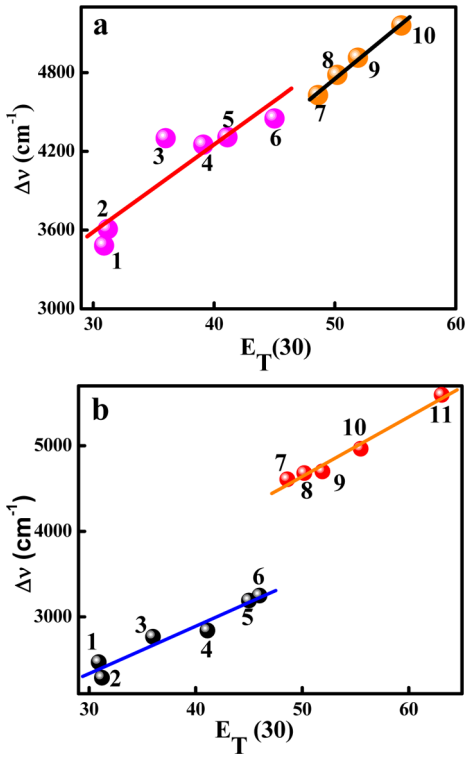

Figure 11. Plot of Stokes shift ($\Delta\nu$) against Reichardt solvent polarity parameter $E_T(30)$ for (a) DDBHP (1→10; *n*-hex, CY, DOX, $CHCl_3$, DCM, DMSO, ^{i}PrOH, BuOH, EtOH, and MeOH solvents, respectively) and (b) DEASH (1→11; *n*-hex, CY, DOX, DCM, DMSO, ACN, ^{i}PrOH, BuOH, EtOH, MeOH, and H_2O solvents, respectively) molecules.

parameter (α)[15,17] for protic solvents, and this is shown in Figure 10a (inset). The linear nature of the plot suggests that the CT band in protic solvents is influenced by the hydrogen bonding interaction. Similar results have been found in the case of the DEASH molecule and are shown in Figure 10b and its inset. As seen in Figure 11a, for DDBHP, the plot of Stokes shift versus solvent polarity parameter $E_T(30)$[58] generates two straight lines with different slopes: one for the nonpolar, polar aprotic solvents, and the other for the polar protic solvents. This plot clearly indicates that two types of interactions are present: in aprotic solvents only dipolar interactions are present, whereas in protic solvents both the dipolar and hydrogen bonding interactions are present. A similar type of plot for DEASH also generates two straight lines (Figure 11b): one for nonpolar, polar aprotic solvents, and another for hydrogen bonding solvents.

3.6. Analysis of Fluorescence Quantum Yield. The observed fluorescence quantum yields of DDBHP and DEASH at room temperature with variation of polarity and hydrogen bonding ability of the solvents are presented in Table 1. DDBHP shows very high quantum yield in nonpolar and hydrogen bonding solvents but comparatively low quantum yield for polar aprotic solvents such as DOX, dimethylformamide (DMF), dimethyl sulfoxide (DMSO), ACN, and so on (Table 1). In polar protic solvents (except H_2O), hydrogen bonding effect has showed greater influence on the quantum yield and this overcomes the polarity effect. The exception in quantum yield of DDBHP in water medium may be due to the acidic nature of the triple distilled water (pH = 5.8) as DDBHP shows very low emission intensity in acidic pH.[16,17] On the other hand, for DEASH, a similar trend of quantum yields is observed for hydrogen bonding solvents, and it is higher compared to that of the nonpolar and polar aprotic solvents. Other than hydrogen bonding solvents, quantum yields of DEASH are found to be low compared to the quantum yields of DDBHP. For the DEASH molecule, quantum yields in nonpolar solvents and other polar solvents vary within the range 0.10−0.30. The reported quantum yield data in nonpolar and polar protic solvents (Table 1) reveals that DDBHP and DEASH have different influences on the polarity of the medium. In nonpolar solvents, the quantum yields of DDBHP are higher, and lower for polar aprotic solvents, whereas the reverse trend was observed in the case of DEASH.

3.7. Analysis of Fluorescence Lifetime. Fluorescence lifetimes have been measured to further investigate the excited state behavior of DDBHP and DEASH molecules. All decay curves have been well fitted by a biexponential decay pattern with acceptable χ^2 values, and time-resolved data are presented in Table 2. The time-resolved data in Table 2 reveals that both DDBHP and DEASH show biexponential decay curves when monitoring at LE, CT, and PT emission maxima. Between the biexponential decay components, the faster component (ps time scale) contributes a higher percentage (99%) with another negligible slower (ns time scale) component (1%). When monitoring LE (high energy emission band), the major contribution arises from the intramolecular hydrogen-bonded closed form for both the compounds, [33] whereas, at CT and PT emission maxima, the major component is obviously due to the CT and PT states, respectively. The origin of the negligible amount of slower component is not clear at all now. When monitoring at the CT emission maxima, both the percentage of τ_1 and τ_2 components are nearly equal (50%) in protic solvents

dx.doi.org/10.1021/jp3079698 | J. Phys. Chem. A 2012, 116, 10948−10958

Table 2. Time-Resolved Data of DDBHP and DEASH in Different Solvents

compound	solvent (λ_{em})	τ_1 (ns)	τ_2 (ns)	a_1	a_2	$\langle\tau\rangle$ (ns)	χ^2
DDBHP	*n*-hex(461)	0.037	0.927	0.984	0.015	0.285	1.18
	CCl_4(456)	0.142	3.719	0.998	0.001	0.308	1.13
	$CHCl_3$(469)	0.108	0.323	0.866	0.133	0.176	1.38
	BuOH(466)	0.070	0.605	0.970	0.029	0.181	1.29
	EtOH(459)	0.043	0.793	0.985	0.014	0.201	1.17
	MeOH(451)	0.024	0.806	0.991	0.008	0.203	1.18
	$CHCl_3$(498)	0.120	0.368	0.743	0.256	0.248	1.24
	DMSO(482)	0.141	3.429	0.998	0.001	0.272	1.12
	BuOH(510)	0.182	0.897	0.567	0.432	0.746	1.20
	EtOH(515)	0.115	0.809	0.485	0.514	0.727	1.21
	MeOH(520)	0.091	0.729	0.447	0.552	0.670	1.20
	BuOH(579)	0.803	3.674	0.980	0.019	1.048	1.18
	EtOH(582)	0.729	3.888	0.984	0.015	0.977	1.19
	MeOH(595)	0.656	3.971	0.986	0.013	0.906	1.30
DEASH	*n*-hex(450)	0.096	0.965	0.948	0.051	0.401	1.03
	DCM(473)	0.242	1.514	0.870	0.129	0.856	1.20
	$CHCl_3$(471)	0.267	3.172	0.993	0.006	0.470	1.08
	DOX(465)	0.212	2.779	0.996	0.004	0.343	1.17
	BuOH(467)	0.086	0.775	0.926	0.073	0.371	1.18
	EtOH(465)	0.055	0.699	0.924	0.075	0.382	1.33
	MeOH(470)	0.025	0.602	0.961	0.038	0.314	1.16
	DCM(504)	0.237	1.530	0.930	0.069	0.658	1.18
	$CHCl_3$(499)	0.274	3.216	0.994	0.005	0.447	1.22
	DOX(487)	0.210	2.933	0.996	0.003	0.329	1.14
	DMF(481)	0.294	3.035	0.995	0.005	0.421	1.22
	BuOH(512)	0.253	0.877	0.499	0.500	0.738	1.41
	EtOH(514)	0.161	0.704	0.408	0.591	0.630	1.19
	MeOH(518)	0.112	0.581	0.346	0.653	0.537	1.28
	DOX(542)	0.210	3.249	0.996	0.004	0.381	1.18
	DMF(553)	0.284	3.790	0.996	0.004	0.469	1.15

Table 3. Spectroscopic Data for Comparative Study between SA, SAA, and DDBHP, DEASH Molecules[a]

	SA[a]	SAA[a]	DDBHP[b]	DEASH[c]
λ_{abs} (nm)	337	355	410	423
λ_{em} (nm)	540	573	595	553
Stokes shift ($\Delta\nu$ cm^{-1})	11200	10720	7583	5557
quantum yield	0.12×10^{-3}	0.7×10^{-3}	504×10^{-3}	76×10^{-3}
life time (τ)	7 ps (keto) < 50 fs (enol)	17 ps (keto) < 50 fs (enol)	906 ps	469 ps

[a]The superscripts a, b, and c represent that data are provided in ACN, MeOH, DMF solvent, respectively. The photophysical data of SA and SAA are provided from ref 33.

where the τ_1 component arises from the LE of the closed form and τ_2 arises from the CT component of DDBHP. Here both the values of τ_1 and τ_2 decrease with increasing hydrogen bonding ability of the solvent. Similar observations were observed in the case of the PT band. However, the lifetime components of the PT band are comparatively higher compared to that of the CT and LE band (Table 2). Overall, the average fluorescence lifetime decreases from 1.048 to 0.906 ns with increasing hydrogen bonding ability of solvents. Therefore we can conclude that hydrogen bonding solvents have an influence on the photophysics of DDBHP. For the DEASH molecule, the major component τ_1 (~98%) follows a trend similar to that of DDBHP (Table 2).

3.8. Comparative Spectral Properties between DDBHP and DEASH. Scheme 1 shows that the DDBHP molecule contains only one −OH group, and DEASH contains two −OH groups. Therefore, there is a possibility of single proton transfer in DDBHP and double proton transfer in the DEASH molecule. However, the reported literature on similar systems[49,52,53] and our experimental results insist that only single proton transfer is observed in DEASH. Due to the symmetric nature of DEASH, it shows very low ground-state dipole moment (0.03 D), whereas DDBHP (asymmetric molecule) shows higher ground-state dipole moment (1.25 D); in the excited state, the dipole moments for DEASH and DDBHP are calculated to be 7.08 and 9.04 D, respectively. DDBHP shows a PT band in polar protic solvents, whereas DEASH shows PT band in polar aprotic solvents (except water). Besides hydrogen bonding solvents, in all cases absorption spectra of DEASH are 10 nm red-shifted compared to the DDBHP (Table 1). The reported quantum yields data in Table 1 demonstrate that in nonpolar and polar protic solvent, DDBHP shows higher quantum yields compared to DEASH.

3.9. Effect of $-NEt_2$ Groups on Photophysical Properties of DDBHP and DEASH. To study the effect of $-NEt_2$ groups on the photophysical properties of these molecules, we

dx.doi.org/10.1021/jp3079698 | J. Phys. Chem. A 2012, 116, 10948−10958

have compared the spectral data of DDBHP and DEASH molecules with other molecular systems that are structurally similar, except with two $-NEt_2$ groups. The molecule SAA is structurally similar (Scheme S2a) to DEASH (without two $-NEt_2$ groups), but we did not find any reported molecule that is identical to DDBHP, i.e., without two $-NEt_2$ groups. For this reason we have taken the SA molecule (Scheme S2b) for comparison. DDBHP and DEASH molecules show prominent spectral properties compared to SA and SAA molecules. From the data presented in Table 3, it is clear that the absorption band maxima of DDBHP and DEASH molecules shifted to the red side with respect to SA and SAA, and it is mainly due to higher conjugation in the ground state.[33,57,62] As reported in the literature, SA and SAA molecules showed only PT emission,[33,49] but here both the molecules show CT and PT emission depending upon the polarity of the solvent.[36] The reversal of the emission intensity of the PT and CT bands were observed after introduction of $-NEt_2$ groups. SA and SAA molecules showed only an intense PT band, whereas we have observed the PT band with very low intensity and the CT band with very high intensity for both DDBHP and DEASH molecules.[33,57] Therefore, it is clear that the PT band intensity is slightly suppressed by the CT band in the presence of $-NEt_2$ groups in SA and SAA Schiff bases. At the same time, for the same reason, the quantum yields and lifetimes are enhanced many times for both the compounds with respect to SA and SAA (Table 3).[33] The Stokes shift for the PT band also decreases due to introduction of $-NEt_2$ groups.[33]

4. CONCLUSIONS

In conclusion, we report the photophysical properties of two biologically important photochromic Schiff bases, DDBHP and DEASH molecules, in different solvents with variation of polarity and hydrogen bonding ability of solvents. Both compounds show ICT and PT phenomena in the excited state. Redistribution of molecular charge in the excited state was confirmed from the solvatochromic Lippert–Mataga plot and from the calculated high change of excited-state dipole moment from that of the ground-state geometry for DDBHP ($\Delta\mu$ = 8.15 D) and DEASH ($\Delta\mu$ = 7.05 D) molecules. The emission spectral properties and lifetime data clearly show that hydrogen bonding solvents have profound influence on the photophysical properties of both the molecules. Comparison of spectral properties shows that DDBHP have higher quantum yields than DEASH. Effect of introduction of $-NEt_2$ groups to the reported Schiff bases SAA and SA reveals that it enhances the fluorescence lifetime from femtosecond to picosecond time scale. The presence of $-NEt_2$ groups also increases fluorescence quantum yields and decreases the Stokes shift of the PT emission.

■ ASSOCIATED CONTENT

Supporting Information

Supporting Information contains chemicals and solvents used; chemical structure of DEABH, SA, and SAA; excitation spectra of DDBHP and DEASH in different solvents; and the effect of TFA on the absorption and emission spectra of DDBHP and DEASH in ACN solvent. This information is available free of charge via the Internet at http://pubs.acs.org.

■ AUTHOR INFORMATION

Corresponding Author

*E-mail: nguchhait@yahoo.com; Tel: 91-33-23508386; Fax: 91-33-23519755.

Notes

The authors declare no competing financial interest.

■ ACKNOWLEDGMENTS

N.G. gratefully acknowledges the financial support received from the Department of Science and Technology, India (Project No. SR/S1/PC-26/2008). S.J. and S.D. would like to thank UGC for Fellowship.

■ REFERENCES

(1) Fu, Y.; Li, H.; Hu, W. *Eur. J. Org. Chem.* **2007**, *2007*, 2459–2463.
(2) Jana, S.; Dalapati, S.; Alam, M. A.; Guchhait, N. *J. Photochem. Photobiol., A* **2012**, *238*, 7–15.
(3) Jana, S.; Dalapati, S.; Alam, M. A.; Guchhait, N. *Spectrochim. Acta, Part A* **2012**, *92*, 131–136.
(4) Irie, M. *Chem. Rev.* **2000**, *100*, 1683–1684.
(5) Sliwa, M.; Létard, S.; Malfant, I.; Nierlich, M.; Lacroix, P. G.; Asahi, T.; Masuhara, H.; Yu, P.; Nakatani, K. *Chem. Mater.* **2005**, *17*, 4727–35.
(6) Cozzi, P. G. *Chem. Soc. Rev.* **2004**, *33*, 410–421.
(7) Zhuang, X.; Oyaizu, K.; Niu, Y.; Koshika, K.; Chen, X.; Nishide, H. *Macromol. Chem. Phys.* **2010**, *211*, 669–676.
(8) Osowole, A. A. *Int. J. Inorg. Chem.* **2011**, DOI: 10.1155/2011/650186.
(9) Ready, J. M.; Jacobsen, E. N. *Angew. Chem., Int. Ed.* **2002**, *41*, 1374–1377.
(10) Selwin Joseyphus, R.; Sivasankaran Nair, M. *Arabian J. Chem.* **2010**, *3*, 195–204.
(11) Hadjoudis, E.; Mavridis, I. M. *Chem. Soc. Rev.* **2004**, *33*, 579–588.
(12) Ziolek, M.; Kubicki, J.; Maciejewski, A.; Naskrecki, R.; Grabowska, A. *J. Chem. Phys.* **2006**, *124*, 124518–10.
(13) Mitra, S.; Tamai, N. *Phys. Chem. Chem. Phys.* **2003**, *5*, 4647–4652.
(14) Mitra, S.; Tamai, N. *Chem. Phys. Lett.* **1998**, *282*, 391–397.
(15) Grabowski, Z. R.; Rotkiewicz, K.; Rettig, W. *Chem. Rev.* **2003**, *103*, 3899–4032.
(16) Jana, S.; Dalapati, S.; Ghosh, S.; Kar, S.; Guchhait, N. *J. Mol. Struct.* **2011**, *998*, 136–143.
(17) Jana, S.; Ghosh, S.; Dalapati, S.; Kar, S.; Guchhait, N. *Spectrochim. Acta, Part A* **2011**, *78*, 463–468.
(18) Lai, R. Y.; Fabrizio, E. F.; Lu, L.; Jenekhe, S. A.; Bard, A. J. *J. Am. Chem. Soc.* **2001**, *123*, 9112–9118.
(19) He, C.; He, Q.; He, Y.; Li, Y.; Bai, F.; Yang, C.; Ding, Y.; Wang, L.; Ye, J. *Sol. Energy Mater. Sol. Cells* **2006**, *90*, 1815–1827.
(20) Jana, S.; Dalapati, S.; Ghosh, S.; Guchhait, N. *J. Photochem. Photobiol., B* **2012**, *112*, 48–58.
(21) Jana, S.; Ghosh, S.; Dalapati, S.; Guchhait, N. *Photochem. Photobiol. Sci.* **2012**, *11*, 323–332.
(22) Jana, S.; Dalapati, S.; Ghosh, S.; Guchhait, N. *J. Photochem. Photobiol., A* **2012**, *231*, 19–27.
(23) Jana, S.; Dalapati, S.; Ghosh, S.; Guchhait, N. *Biopolymers* **2012**, *97*, 766–777.
(24) Rullière, C.; Grabowski, Z. R.; Dobkowski, J. *Chem. Phys. Lett.* **1987**, *137*, 408–413.
(25) Beens, H.; Grellmann, K. H.; Gurr, M.; Weller, A. H. *Spec. Discuss. Faraday Soc.* **1965**, *39*, 183–193.
(26) Petek, H.; Zhao, J. *Chem. Rev.* **2010**, *110*, 7082–7099.
(27) Hammes-Schiffer, S.; Stuchebrukhov, A. A. *Chem. Rev.* **2010**, *110*, 6939–6960.
(28) Huynh, M. H. V.; Meyer, T. J. *Chem. Rev.* **2007**, *107*, 5004–5064.
(29) Kasha, M. *J Chem. Soc., Faraday Trans. 2* **1986**, *82*, 2379–2392.

(30) Catalán, J.; Díaz, C.; Pérez, P.; de Paz, J. L. G. *J. Phys. Chem. A* **2006**, *110*, 9116−9122.
(31) Lochbrunner, S.; Wurzer, A. J.; Riedle, E. *J. Chem. Phys.* **2000**, *112*, 10699−10702.
(32) Yahagi, T.; Fujii, A.; Ebata, T.; Mikami, N. *J. Phys. Chem. A* **2001**, *105*, 10673−10680.
(33) Ziolek, M.; Kubicki, J.; Maciejewski, A.; Naskrecki, R.; Grabowska, A. *Phys. Chem. Chem. Phys.* **2004**, *6*, 4682−4689.
(34) Mitra, S.; Tamai, N. *Chem. Phys.* **1999**, *246*, 463−475.
(35) Hammud, H. H.; Ghannoum, A.; Masoud, M. S. *Spectrochim. Acta, Part A* **2006**, *63*, 255−265.
(36) Joshi, H.; Kamounah, F. S.; Gooijer, C.; van der Zwan, G.; Antonov, L. *J. Photochem. Photobiol., A* **2002**, *152*, 183−191.
(37) Ohshima, A.; Momotake, A.; Arai, T. *J. Photochem. Photobiol., A* **2004**, *162*, 473−479.
(38) Ortiz-Sanchez, J. M.; Gelabert, R.; Moreno, M.; Lluch, J. M. *J. Chem. Phys.* **2008**, *129*, 214308−214311.
(39) Rodríguez-Córdoba, W.; Zugazagoitia, J. S.; Collado-Fregoso, E.; Peon, J. *J. Photochem. Photobiol., A* **2007**, *111*, 6241−6247.
(40) Harada, J.; Fujiwara, T.; Ogawa, K. *J. Am. Chem. Soc.* **2007**, *129*, 16216−16221.
(41) Barbara, P. F.; Rentzepis, P. M.; Brus, L. E. *J. Am. Chem. Soc.* **1980**, *102*, 2786−2791.
(42) Dalapati, S.; Jana, S.; Guchhait, N. *Chem. Lett.* **2011**, *40*, 279−281.
(43) Dalapati, S.; Jana, S.; Alam, M. A.; Guchhait, N. *Sens. Actuators, B* **2011**, *160*, 1106−1111.
(44) Lakowicz, J. R. *Principles of Fluorescence Spectroscopy*; Springer/Plenum: New York, 2006.
(45) Rurack, K. *Fluorescence Quantum Yields: Methods of Determination and Standardization and Quality Assurance in Fluorescence Measurements I*; Resch-Genger, U., Ed.; Springer: Berlin Heidelberg, 2008; Vol. *5*, pp 101−145.
(46) Suresh, M.; Mandal, A. K.; Saha, S.; Suresh, E.; Mandoli, A.; Di Liddo, R.; Parnigotto, P. P.; Das, A. *Org. Lett.* **2010**, *12*, 5406−5409.
(47) Guha, D.; Mandal, A.; Koll, A.; Filarowski, A.; Mukherjee, S. *Spectrochim. Acta, Part A* **2000**, *56*, 2669−2677.
(48) Becker, R. S.; Lenoble, C.; Zein, A. *J. Phys. Chem.* **1987**, *91*, 3509−3517.
(49) Ziółek, M.; Filipczak, K.; Maciejewski, A. *Chem. Phys. Lett.* **2008**, *464*, 181−186.
(50) Mahanta, S.; Singh, R. B.; Kar, S.; Guchhait, N. *Chem. Phys.* **2008**, *354*, 118−129.
(51) Singh, R. B.; Mahanta, S.; Guchhait, N. *J. Photochem. Photobiol., A* **2008**, *200*, 325−333.
(52) Kownacki, K.; Kaczmarek, u. k.; Grabowska, A. *Chem. Phys. Lett.* **1993**, *210*, 373−379.
(53) Kownacki, K.; Mordzinski, A.; Wilbrandt, R.; Grabowska, A. *Chem. Phys. Lett.* **1994**, *227*, 270−276.
(54) Samanta, A.; Paul, B. K.; Mahanta, S.; Singh, R. B.; Kar, S.; Guchhait, N. *J. Photochem. Photobiol., A* **2010**, *212*, 161−169.
(55) Paul, B. K.; Samanta, A.; Guchhait, N. *Photochem. Photobiol. Sci.* **2010**, *9*, 57−67.
(56) Samanta, A.; Paul, B. K.; Kar, S.; Guchhait, N. *J. Fluoresc.* **2011**, *21*, 95−104.
(57) Ziolek, M.; Gil, M.; Organero, J. A.; Douhal, A. *Phys. Chem. Chem. Phys.* **2010**, *12*, 2107−2115.
(58) Reichardt, C. *Chem. Rev.* **1994**, *94*, 2319−2358.
(59) Mataga, N.; Chosrowjan, H.; Taniguchi, S. *J. Photochem. Photobiol., C* **2005**, *6*, 37−79.
(60) Frisch, M. J.; Trucks, G. W.; Schlegel, H. B.; Scuseria, G. E.; Robb, M. A.; Cheeseman, J. R.; Montgomery, J. A.; Vreven, T.; Kudin, K. N.; Burant, J. C. et al. *Gaussian 03*, revision C.02; Gaussian, Inc.: Pittsburgh, PA, 2003.
(61) Sumalekshmy, S.; Gopidas, K. R. *J. Phys. Chem. B* **2004**, *108*, 3705−3712.
(62) Sliwa, M.; Mouton, N.; Ruckebusch, C.; Poisson, L.; Idrissi, A.; Aloise, S.; Potier, L.; Dubois, J.; Poizat, O.; Buntinx, G. *Photochem. Photobiol. Sci.* **2010**, *9*, 661−669.